ELECTRON TEMPERATURE AND DENSITY OF THE TOPSIDE EQUATORIAL IONOSPHERE AS OBTAINED FROM A THEORETICAL MODEL

K.K. Chetia[1], A. Borgohain[2] and P. K. Bhuyan[3]

[1]Department of Physics Dibrugarh University, Dibrugarh 786004 India, e-mail: kallul555@yahoo.co.in

[2]As (1), above, e-mail: arupgohain@yahoo.com

[3]As (1), above, Email: bhuyan@dibru.ernet.in

ABSTRACT

The electron density and temperature distribution of the equatorial and low latitude ionosphere along 75°E has been investigated by simultaneously solving the continuity and momentum equations of ion and electron flux along geomagnetic field lines from the northern to the southern hemisphere. Model results are also compared with electron density and electron temperature measured in situ by the Indian SROSS C2 satellite at an altitude of ~ 500 km within the latitude belt of 31° S to 34° N and 70°±30° E longitude sector. The model simulates the EIA in density and morning temperature enhancements.

INTRODUCTION

The distribution of plasma in the ionosphere F region depends on the three processes of production, loss and transport. At equatorial and low latitudes, the F region is characterized by a depression in ionization densities at the magnetic equator and two maximum on either side of the equator. Besides this well-known phenomenon of equatorial ionization anomaly, the equatorial ionosphere is known to exhibit some unique features such as the equatorial electrojet, the spread-F etc. The horizontal orientation of the geomagnetic fields line at the equator and shift between the geographic and geomagnetic equator is known to be the main reason for observation of these features and their longitudinal variation. The E region eastward electric field at the equator causes the F region plasma to drift upward during the daytime. As the plasma is lifted to greater height, it diffuses downward along geomagnetic field lines under the twin action of gravity and pressure gradients. A plasma fountain thus forms which moves ionization from the equator to the two anomaly crests. After sunset, the electric field reverses in direction and the F-region plasma drifts downward. The fountain reverses and the crests disappear. The location of the two anomaly peaks shifts towards higher latitudes with increase in EXB drift velocity. Asymmetric neutral winds about the equator produce a north south asymmetry in the EIA. The latitudinal extent of the crests also varies with solar and magnetic activity. The fountain rises to several hundred kilometers at the equator and the crests become weaker with increase in altitudes. At higher altitudes, a single crest of ionization forms over the equator.

Many attempts have been made in the past to theoretically investigate the dynamics of the low latitude ionosphere. Balan et al [1] have found that the north-south asymmetries of the equatorial plasma fountain and equatorial anomaly are more dependent upon the displacement of the geomagnetic equator from the geographic equator. Watanabe et al. [2] had used a time dependent three dimensional simulation procedure to study the variation of electron and ion temperature and density within ±30° and 200 km to 1000 km altitude region. Their results show that the structure of the equatorial ionospheric F region is strongly affected by the plasma drift, which is induced by the ionospheric electric field, neutral wind, exospheric temperature and intensity of solar flux variations. Balan et al [3] theoretically described a plasma temperature anomaly in the equatorial topside ionosphere. Bhuyan and Kakoty [4] [5] have simulated the ion density distribution in topside F region of the Indian low latitude ionosphere for solar minimum equinoctial conditions and compared the results with the density measurements made by the Indian SROSS C2 satellite. The simulations reproduced the well known equatorial anomaly(EIA) in electron density at the peak of the F-2 region in the Indian low latitude sector during solar minimum. At an altitude of ~500 km, both the model generated and SROSS C2 observed electron density did not show the EIA. A weak E×B during solar minimum may be responsible for absence of this anomaly either in the equinoxes or December and June solstices. The simulated O^+ density, which is the major ion around F peak heights, exhibited a minimum around pre-sunrise hours and a maximum during daytime. On the other hand, H^+ density is found to be higher at nighttime and lower during the day. Bhuyan et al. [4] [5] [6] have found that the model parameters are sensitive to the initial conditions and the three input parameters photo ionization, neutral wind and E×B vertical drift velocity.

THE MODEL

Continuity, Momentum and Energy Balance Equations

The continuity and momentum equation of ion and electron flux are simultaneously solved along geomagnetic field lines from the Northern to the Southern Hemisphere for F region ionosphere. The effects of E×B drift, horizontal wind, magnetic field, solar activity and chemical reactions are considered for the calculation of density. Heating due to photoelectrons, collision between ions, ions and electrons, rotational heat transfer, vibrational heat transfer and thermal conductivity are considered for calculation of electron and ion temperature. The following equations are solved for low solar activity equinoctial conditions.

$$\frac{\partial N}{\partial t} = P - L - \nabla.(N\,V) \tag{1}$$

$$v_{ll} = h_{ij} v_j + h_{in} v_n - D_i \left[\begin{array}{l} \dfrac{1}{N_i}\dfrac{\partial N_i}{\partial s} + \dfrac{T_e}{T_i N_e}\dfrac{\partial N_e}{\partial s} - \dfrac{m_i}{kT_i} g_{ll} + \\ \dfrac{1}{T_i}\left(\dfrac{\partial}{\partial s}(T_e + T_i) + \beta_i \dfrac{\partial T_i}{\partial s} - \beta_{ij}\dfrac{\partial T_j}{\partial s} \right) \end{array} \right] \tag{2}$$

$$\frac{3}{2} k N_i \frac{DT_i}{Dt} = Q_i - kN_i.T_i.\nabla.\vec{v}_i + \nabla.\left(\kappa_i \nabla T_i\right) + F_{in} \tag{3}$$

Here, N is the ion density, P and L are the ion production and ion loss rates respectively and V is the ion transport velocity. The momentum equation for the i^{th} ion, as given by Moffett et al. [7] gives the form of the field-aligned ion velocity used in the model. Equation (3) represents the energy balance equation for the i^{th} constituent (where i=O^+,H^+, or e).Where Q_i gives heating rate (positive or negative) due to collisional interactions with other ion or neutral species, the second and third terms on the right hand side are due to adiabatic heating/cooling and thermal conductivity respectively. κ_i (eVm $^{-1}$ $s^{-1}K^{-1}$) is the thermal conductivity for i^{th} ion is given by Banks and Kockarts[8].Also the thermal conductivity κ_e for electrons is given by Schunk and Nagy[9]. F_{in} is the frictional heating due to the relative motion between the i^{th} ion and neutral gases. The production of O^+ is assumed due to both photo ionization and chemical process. The production of H^+ is considered only due to the resonant charge exchange reaction with oxygen Stubbe[10].The chemical reaction rates are as given by Raitt et al.[11] whereas the rate coefficients for loss of O^+ following charge exchange reactions with O_2 and N_2 are taken from Torr and Torr[12]. The production of O^+ due to photo ionization is given by.

$$P_{photo} = \sum_{\lambda} \Phi(\lambda)\sigma^i(\lambda)\left[O\right]\exp\left[-\sum_j \sigma_j^a(\lambda) n_j H_j Ch_j(\chi)\right] \tag{4}$$

where the summation $\sum_{\lambda}$ is over the wavelength range of the ionizing radiation and $\sum_j$ denotes a summation over the neutral gases O, O_2 and N_2. The solar EUV radiation flux intensities, $\Phi(\lambda)$,are taken from Schunk and Nagy[9], as are the ionization and absorption cross sections(σ^i and σ^a respectively). The Chapman grazing incidence function $Ch_j(\chi)$ for the j^{th} neutral gas, as approximated by Rishbeth and Garriott[13]

E×B Drift and Neutral Wind.

The upward drift velocity induced by the ionospheric electric field for equinox conditions is modeled as

$$V_{up} = 20\times\cos\left(\left(LT-11\right)\frac{\pi}{12}\right) + \frac{40\times\exp\left[-\left(LT-19\right)^2/3\right]}{1+\exp\left[\left(h-1000\right)/300\right]} - 10\times\left(\begin{array}{l}\exp\left[-\left(LT-4\right)^2/16\right] \\ +\exp\left[-\left(LT-21\right)^2/16\right]\end{array}\right)\ ms^{-1} \tag{5}$$

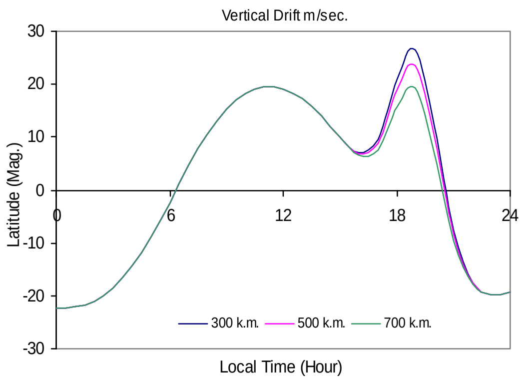

Fig. 1 E×B drift as a function of LT and magnetic latitude at three different heights

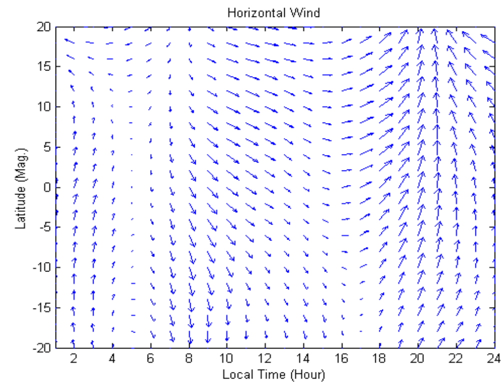

Fig.2 The Horizontal wind as a function of LT and magnetic latitude

on the basis of radar observation in [14], where LT is local time in hour and h is height in kilometers. We have used the thermospheric wind model HWM90 [15] to obtained the neutral wind inputs. HWM90 gives meridonal and zonal wind velocities as a function of altitude, latitude longitude and solar activity for all time of the day. Fig. 1 and Fig. 2 respectively show the plasma drift and neutral wind models used in the simulation.

Neutral atmosphere and Temperature

The concentrations of the atmospheric neutral constituents O, O_2, N_2, H, and the neutral gas temperature are calculated from the MSIS-86 thermospheric model [16] as a function of altitude, latitude and local time.

RESULT AND DISCUSSION

The continuity equation, momentum equation, energy balance equations are solved simultaneously for solar minimum equinoctial conditions for the tilted dipole magnetic field lines. Fig. 3 and Fig. 4 show the three dimensional simulation results of electron density and electron temperatures respectively at a fixed altitude of 500 km. The simulated electron density has a minimum around pre-sunrise hours and a maximum during noontime. The model also reproduce equatorial ionization anomaly at F peak heights of 300 km. The model reproduces morning and evening enhancement of electron temperature observed at F region heights. It is observed that the E×B drift and neutral wind modulate amplitude and the position of the EIA. The model result is compared with the data measured by Indian SROSS C2 satellite at this region during the low solar activity period of 1995. The average height of the satellite was 500 km and it covered the latitude belt of -31° to 34°. The electron density profile given by the model and that measured by the SROSS C2 are similar. We observed that the electron density forms a minimum (~$1\times10^{11}m^{-3}$) during sunrise (04:00-06:00 LT) and daytime density reach a maximum level of $9\times10^{11}/m^3$, which is almost similar to the observed data from SROSS C2 satellite. SROSS C2 observations indicate that in low solar activity period electron density at 500 km shows asymmetric EIA. In the equinoxes, electron density maximizes at 10°N and 5°S and the anomaly peak is higher in the northern hemisphere compared to that in the southern hemisphere. The crest to trough ratio in observed Ne is 1.5 and 1.25 in northern and southern hemispheres respectively. The measured electron temperature from SROSS C2 varies between 700 K and 800 K during nighttime (20:00-04:00 LT), rises sharply during sunrise (04:00-06:00 LT) to reach a level of ~ 3500 K within a couple of hours and then falls to the average day time temperature of 1600 K. A secondary maximum is observed around 16:00-18:00 LT where electron temperature reaches a high value of ~ 2000K. However the model simulates morning Te at ~2900 K which is lower than the observed morning maximum. The model daytime temperature is around 1500 K and evening enhancement temperature is ~1700 K. The morning enhancement in electron temperature is due to low electron densities and photoelectron heating. In the evening, due to horizontal wind the density of neutral species (H, H_2, O, N_2 etc) increases and another maximum occurs.

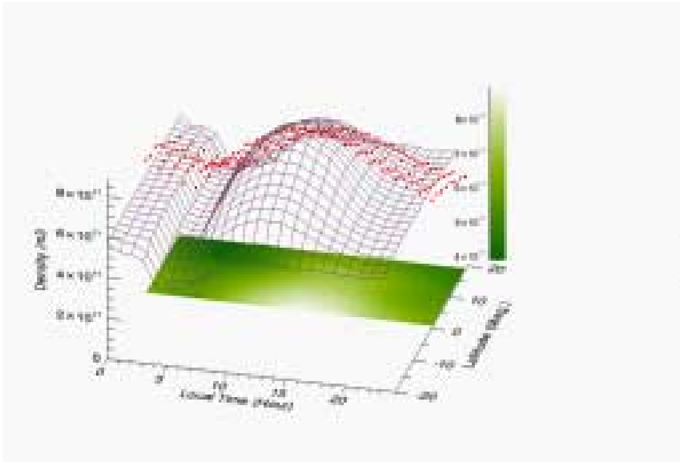

Fig. 3 Comparison between simulated electron density at 500 km altitude and the electron density observed by SROSS C2. The red dots and green contour plot show observed data, and the wire mesh shows simulated data

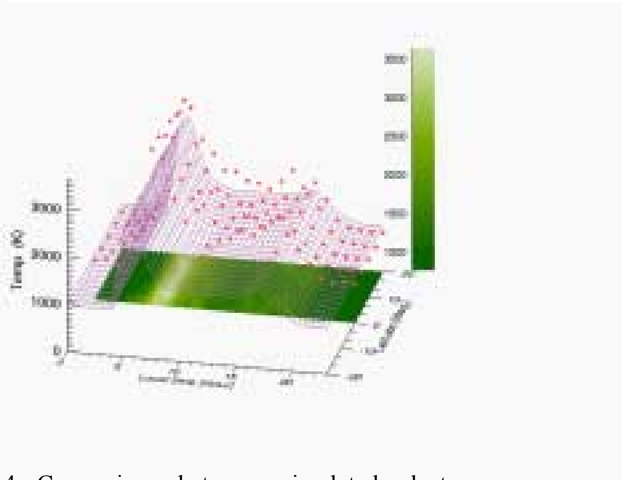

Fig 4 Comparison between simulated electron temperature at 500 km altitude and the electron density observed by SROSS C2. The red dots and green contour plot show observed data, and the wire mesh shows simulated data

ACKNOWLEDGEMENT

This work was carried out with a grant (10/2/298) received from the Indian Space Research Organization

REFERENCES

[1] Balan, N., Oyama, K. I., Bailey, G. J., Abdu, M. A., Oyama, K. I., Richards, P. G., MacDougall, J., and Batista, I. S.: equatorial plasma fountain and its effects over three locations: Evidence for an additional layer, the F2-layer, I. S., *J. geophys. Res.,* 102, 2047-2056, 1997a

[2] Watanabe, S, Oyama, K. I. and M A Abdu: Computer simulation of electron and ion densities and temperatures in the equatorial F region and comparison with Hinotori results, *J. Geophys. Res.*100,14581-14590, 1995a

[3] Balan, N., Oyama, K. I., Bailey, G. J., Fukao, S., Watanabe, S., Abdu, M. A.: A plasma temperature anomaly in the equatorial topside ionosphere, *J. Geophys. Res.,* 102, 7485-7492, 1997b.

[4] Bhuyan, P. K. and Kakoty, P. K.: Modelling study of Indian low latitude ionosphere: Part I-Description of the model, *Ind. J. Radio. Space Phys.,* 30, 59-65, 2001a.

[5] Bhuyan, P. K. and Kakoty, P. K.: Modelling study of Indian low latitude ionosphere: Part II-Results and comparison with SROSS c2 satellite data, *Ind. J. Radio. Space Phys.,* 30, 66-71, 2001b.

[6] Bhuyan, P. K. and Kakoty, P. K.: Theoretical simulation of O^+ and H^+ densities in the Indian low latitude F-region and comparison with observations, *Annales Geophysicae,* 20, 1959-1966, 2002

[7] Moffet, R. J., Bailey, G. J., Quegan, S., Rippeth Y., Samson, A. M. and Sellek, R., Phil. *Trans. R. Soc.London.,* 328, 255, 1989.

[8] Banks, P. M. and Kockarts, G., Aeronomy, *Academic Press,* New York, 1973.

[9] Schunk, R. W. and Nagy A. F.: Electron temperatures in the F region of the ionosphere: Theory and observations *Rev. Geophys. Space Phys.,* 16, 355,1978

[10] Stubbe, P., Simultaneous Solution of the Time Dependent Coupled Continuity Equations, Heat Conduction Equatuons and Equations of Motion for a system consisting of a Neutral Gas, An Electron Gas and A forur component Ion Gas, *J. Atmos. Terr. Phys*, 32, 865, 1970.

[11] Raitt, W. J., Schunk, R. W., Banks, P. M.: A comparison of the temperature and density structure in high and low speed thermal proton flow, *Planet. Space Sci,* 23, 110,1975.

[12] Torr, D. G., and Torr M. R: Chemistry of the thermosphere and ionosphere, *J. Atmos. Terr. Phys.,* 41, 797,1979.

[13] Rishbeth, H. and garriott O. K, Introduction to Ionospheric Physics, Academic Press, 138, 1969.

[14] Fejer, B. G., *The equatorial ionosphere electric fields: A review,* , *J. Atmos. Terr. Phys,* 43, 377-386,1981.

[15] Hedin, A. E. et al, Revised Global Model of Thermosphere winds using Satellite and Ground-Based Observations, *J. Geophys. Res.,* 96, 7657,1991.

[16] Hedin, A. E., MSIS-86 thermospheric model, *J. Geophys. Res.,* 92, 4649-4662,1987.